CrossMark

Wet chemical synthesis of zinc-iron oxide nanocomposite

Honami Ito[1] · Shota Amagasa[1] · Naoki Nishida[1] ⬥ ·
Yoshio Kobayashi[2,3] · Yasuhiro Yamada[1]

Abstract Zinc-iron oxide nanoparticles ($Zn_xFe_{3-x}O_4$ and δ-$Zn_xFe_{1-x}OOH$) were success-
fully synthesized by room temperature chemical reaction of a solution containing $ZnCl_2$
and $FeCl_2$ in the presence of gelatin. The composition of products could be controlled
by variation of the Zn/Fe mixture ratio of the starting material. $Zn_xFe_{3-x}O_4$ nanoparti-
cles were obtained from a solution with a high Zn/Fe ratio, whereas Zn-doped feroxyhyte
(δ-$Zn_xFe_{1-x}OOH$) nanoparticles were obtained from a solution with a low Zn/Fe ratio.
The $Zn_xFe_{3-x}O_4$ nanoparticles were spherical with diameters of approximately 10 nm,
and the δ-$Zn_xFe_{1-x}OOH$ particles were needle-like with lengths of approximately 100 nm.
Mössbauer spectra measured at room temperature indicated superparamagnetic behavior of
the nanoparticles, whereas the magnetic components were observed at low temperature. The
Zn content of the intermediate species ($Zn_x^{II}Fe_{1-x}^{II}Fe_2^{III}O_4$) plays an important role in the
oxidation process. When the Zn concentration was high, the content of Fe^{2+} in the interme-
diate species was small, and Zn^{2+} prevented further oxidation of the nanoparticles. When
the starting material had low Zn concentration, the amount of Fe^{2+} in the intermediate
species became large and was rapidly oxidized into δ-$Zn_xFe_{1-x}OOH$ while rinsing under
the ambient atmosphere.

✉ Naoki Nishida
  nnishida@rs.tus.ac.jp

1 Department of Chemistry, Tokyo University of Science, 1-3 Kagurazaka, Shinjuku-ku,
   Tokyo 162-8601, Japan

2 Department of Engineering Science, The University of Electro-Communications,
   1-5-1 Chofugaoka, Chofu, Tokyo 182-8585, Japan

3 Nishina Center for Accelerator-Based Science, RIKEN, 2-1 Hirosawa,
   Wako, Saitama 351-0198, Japan

⌀ Springer

1 Introduction

The magnetic properties of iron oxide nanoparticles doped with other metals are important, particularly with respect to the magnetic properties of nonmagnetic-zinc-doped iron oxide nanoparticles. The magnetic structure of zinc-doped iron oxides can be controlled by varying the amount of zinc doping, whereby the magnetization and hyperfine magnetic fields are decreased with an increase in the amount of zinc doping [1–3]. However, when a very small amount of Zn is doped in an iron oxide, the magnetization increases with respect to that for non-doped iron oxide nanoparticles [1, 3]. Iron(III) oxide-hydroxide (FeOOH) has four crystal structures, α-FeOOH, β-FeOOH, γ-FeOOH, and δ-FeOOH. α-, β- and γ- FeOOH have antiferromagnetic behavior, while δ-FeOOH has ferromagnetic behavior [4]. Thus, δ-FeOOH nanoparticles have potential applications as catalysts and exhibit unique magnetic properties based on size or shape effects [5, 6]. However, δ-FeOOH is not available in nature and is difficult to synthesize artificially. We have previously reported the synthesis of δ-FeOOH nanoparticles by a simple wet chemical method [7]. δ-FeOOH nanoparticles were typically prepared by the rapid oxidation of $Fe(OH)_2$ with H_2O_2, and δ-FeOOH nanoparticles were formed by the rapid oxidation of Fe_3O_4 while rinsing under the ambient atmosphere. Fe_3O_4 nanoparticles doped with other metals can also be synthesized by this method, which can then be rapidly oxidized to δ-FeOOH nanoparticles doped with other metals.

In this work, we examined the synthesis of zinc-iron oxide nanocomposite ($Zn_xFe_{3-x}O_4$ nanoparticles and δ-$Zn_xFe_{1-x}OOH$ nanoparticles) using a wet chemical method. The products were characterized using inductively coupled plasma-atomic emission spectrometry (ICP-AES), powder X-ray diffraction (XRD), transmission electron microscopy (TEM), and Mössbauer spectroscopy.

2 Experimental

Particles were prepared using a modified hydrazine reduction system under the ambient atmosphere at room temperature [7, 8]. The synthesis was performed by starting with a mixture of $ZnCl_2$ and $FeCl_2 \cdot 4H_2O$ with various molar ratios of Zn/Fe. Five samples (S73, S64, S55, S46, and S37) were prepared by employing initial mixtures with Zn/Fe = 7/3, 6/4, 5/5, 4/6 and 3/7, respectively. In this synthesis, 0.4 g of gelatin was completely dissolved in 50 mL of pure water. Then, 2.3 g of $Na_2C_4H_4O_6 \cdot 2H_2O$ and a mixture of $ZnCl_2$ and $FeCl_2 \cdot 4H_2O$ (10 mmol in total metal salt) were added in order. The pH of this solution was subsequently adjusted by the addition of 3 g of NaOH. The solution was left to stand for 10 min in order to dissolve the reagents completely, after which 15 mL of a 10 M aqueous $N_2H_4 \cdot H_2O$ solution was added slowly to the mixture under ultrasonication (100 W, 42 kHz). Then, the mixture was placed under ultrasonication for 40 minutes and left standing for 60 minutes. After the supernatant was removed, the precipitates obtained were collected by centrifugation, rinsed with water and ethanol. As a final step, the precipitate was dried in a vacuum desiccator. The product samples were characterized using ICP-AES (SII Nanotechnology, SPS3520UV), XRD (Rigaku, RINT2500, operated at 50 kV/300 mA), TEM (JEOL, JEM-2100, operated at 200 kV), and Mössbauer spectroscopy (^{57}Co/Rh source).

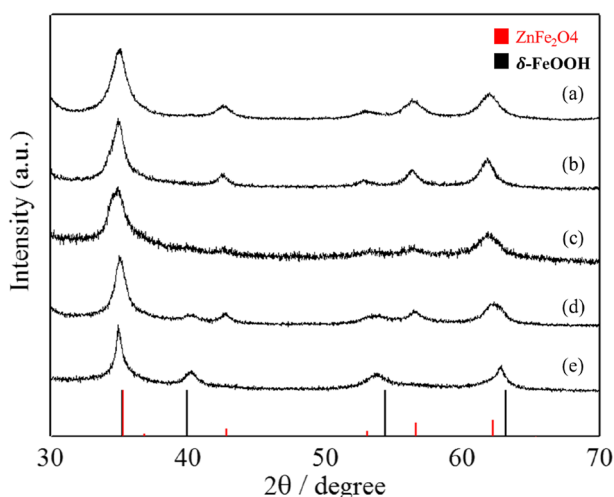**Fig. 1** XRD patterns for the (**a**) S73, (**b**) S64, (**c**) S55, (**d**) S46, and (**e**) S37 samples synthesized from mixtures of Zn/Fe = 7/3, 6/4, 5/5, 4/6 and 3/7, respectively

3 Results and discussion

Figure 1 shows XRD patterns for five samples. The XRD patterns of S73 (Fig. 1a) and S64 (Fig. 1b), which were synthesized with high Zn concentrations, exhibited peaks of $ZnFe_2O_4$ (JCPDS Card No. 22-1012) or Fe_3O_4 (JCPDS Card No. 19-629). $ZnFe_2O_4$ and Fe_3O_4 have very similar patterns. As the amount of the initial Zn salt was decreased, peaks of δ-FeOOH (JCPDS Card No. 13-87) appeared in S46 (Fig. 1d). The peaks of δ-FeOOH in S55 (Fig. 1c) were not significant, but trace peaks of δ-FeOOH were observed by magnifying the intensity of the XRD pattern. In the sample synthesized with the lowest Zn concentration (S37), only δ-FeOOH peaks were observed (Fig. 1e). Peaks of metallic Zn and zinc oxide were absent in all the samples. The observed peaks ($ZnFe_2O_4$ or Fe_3O_4 and δ-FeOOH) were broad, which indicated that the crystallite size of the samples was small. The average crystallite sizes of $ZnFe_2O_4$ or Fe_3O_4 (S73 and S64) were estimated based on the width of the (311) peak and the Scherrer equation to be 6 nm and 7 nm, respectively. The average crystallite sizes of δ-FeOOH (S37) was estimated to be 11 nm based on the width of the (100) peak.

The entire Zn and Fe contents of the samples were determined by ICP-AES measurements, and the correlation between the molar ratios of Zn/Fe measured by ICP and those of the starting materials are shown in Fig. 2. The ICP results showed that all samples contained Zn atoms, although metallic Zn or zinc oxide was not observed by XRD; therefore, the Zn atoms were doped into the Fe_3O_4 or δ-FeOOH nanoparticles. The amounts of Zn estimated by ICP measurements were almost 18% of the nominal ratios of the starting materials, which indicates that almost 82% of Zn atoms were lost from the sample during synthesis. Furthermore, the yield of Zn slightly decreased to 13% of the initial Zn content for the initial mixture with the highest ratio Zn/Fe = 7/3. Although the ideal zinc ferrite ($ZnFe_2O_4$) should have a molar ratio Zn/Fe = 0.5, it was saturated at approximately Zn/Fe = 0.3 in this study. It has been reported that the Zn/Fe molar composition ratio can be limited by the synthesis method [3].
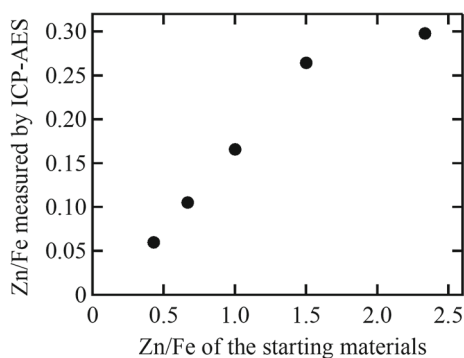
Fig. 2 Relationship between the Zn/Fe molar ratios of the nanoparticles measured using ICP-AES and the nominal molar ratios of the starting materials
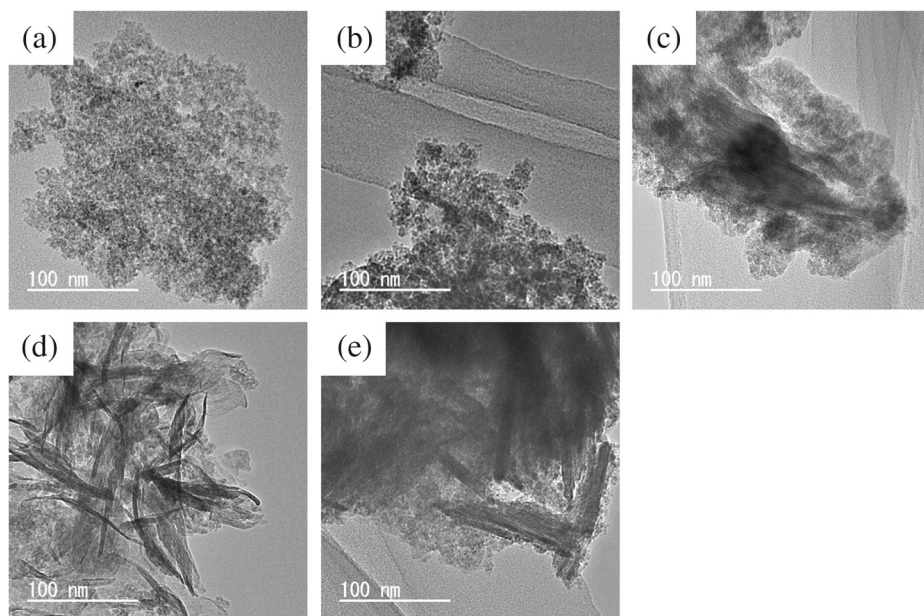

Fig. 3 TEM images of the (**a**) S73, (**b**) S64, (**c**) S55, (**d**) S46, and (**e**) S37 samples

Figure 3 shows TEM images of the five samples. The nanoparticles synthesized with high Zn concentrations (S73 and S64) were spherical with diameters of ca. 10 nm, which was in agreement with the XRD results. Needle-like particles around 100 nm in length appeared as the Zn concentration was decreased (S55 and S46). In the sample synthesized with the lowest Zn concentration (S37), only needle-like particles around 100 nm in length were observed. The XRD pattern for S37 showed broad peaks and the particle size was estimated to be 11 nm assuming a spherical shape; however it became obvious that these crystals were needle-like, and it was not adequate to assume a spherical shape for size estimation using the Scherrer equation. In previous reports, $Zn_xFe_{3-x}O_4$ nanoparticles are typically spherical and δ-FeOOH nanoparticles are reported to be needle-like [1, 5].
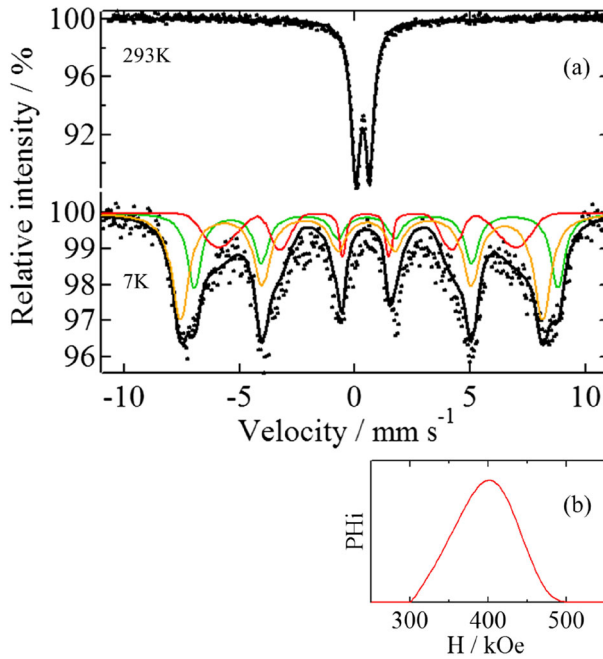
Fig. 4 **a** Mössbauer spectra for S64 measured at 293 K and 7 K, and (**b**) the hyperfine magnetic field distribution

Table 1 Mössbauer parameters obtained at 293 K and 7 K for S64 synthesized with a Zn/Fe molar ratio of 6/4

Temperature K	Component	δ mm s^{-1}	ΔEq mm s^{-1}	H kOe	Γ mm s^{-1}	Yields %
293	$Zn_xFe_{3-x}O_4$	0.32(0)	0.61(0)		0.66(3)	100
7	$Zn_xFe_{3-x}O_4$ (DHMF)	0.49(3)	0.06(7)	402*		21.5
	$Zn_xFe_{3-x}O_4$ (i)	0.39(6)	−0.22(13)	486(1)	0.88(7)	49.5
	$Zn_xFe_{3-x}O_4$ (ii)	0.70(8)	0.42(16)	488(1)	0.73(10)	29.0

*mode of the distributed hyperfine magnetic fields (DHMF)

Mössbauer spectra of S64 acquired at 293 and 7 K are shown in Fig. 4a, and the parameters are summarized in Table 1. The spectrum acquired at 293 K showed a doublet, which could result from the superparamagnetic behavior of the small nanoparticles. The Mössbauer spectrum at 7 K exhibited two sets of sextets and a component with distributed hyperfine magnetic fields (DHMF). The Mössbauer spectrum of Fe_3O_4 generally has multiple components below the Verwey transition, and the spectrum becomes complex due to the overlap of absorptions. The Mössbauer spectrum of bulk Fe_3O_4 at 4.2 K exhibited six sets of sextets; one of these corresponds to the tetrahedral (A) sites, and the remaining five correspond to the octahedral (B) sites [9]. It was also reported that the Mössbauer spectrum of bulk Fe_3O_4 at 85 K had two sets of sextets, one of which corresponds to Fe^{3+} in A and
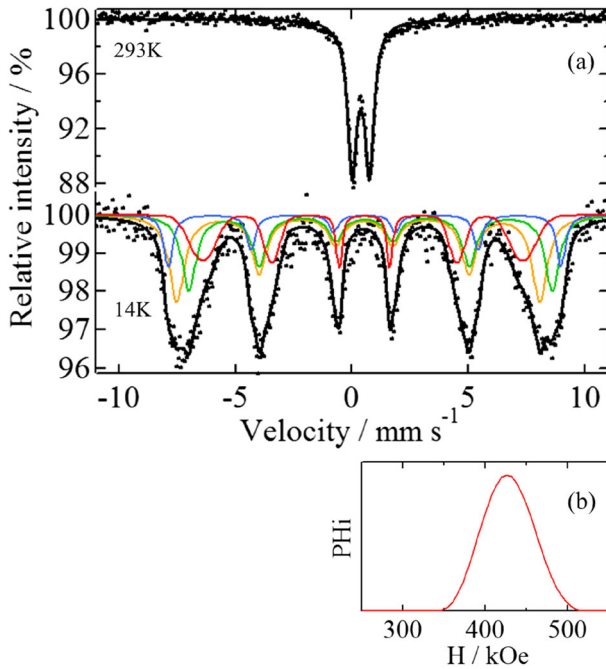
Fig. 5 **a** Mössbauer spectra for S55 measured at 293 K and 14 K, and (**b**) the hyperfine magnetic field distribution

Fig. 6 Mössbauer spectra for S37 measured at 293 K and 7 K
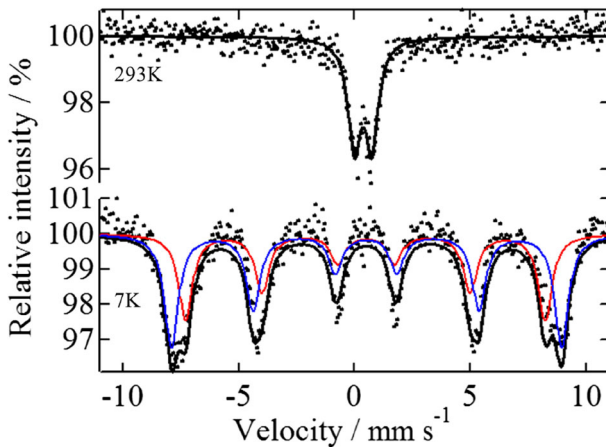
B sites, and the other which corresponds to Fe^{2+} in B sites [10]. Zn^{2+} was reported to possibly occupy both A and B sites, and which sites Zn^{2+} actually occupies is dependent on the amount of Zn doped and the synthesis method [1, 2, 11, 12]. In the Mössbauer spectrum of S64 at 7 K (Fig. 4a), two sextets, i and ii, correspond to the A and B sites of the zinc

Table 2 Mössbauer parameters obtained at 293 K and 14 K for S55 synthesized with a Zn/Fe molar ratio of 5/5

Temperature K	Component	δ mm s^{-1}	ΔEq mm s^{-1}	H kOe	Γ mm s^{-1}	Yields %
293	$Zn_xFe_{3-x}O_4$	0.37(0)	0.73(0)		0.56(1)	100
	$\delta-Zn_xFe_{1-x}OOH$					
14	$Zn_xFe_{3-x}O_4$ (DHMF)	0.49(2)	−0.07(4)	426*		23.0
	$Zn_xFe_{3-x}O_4$ (i)	0.39(15)	0.25(30)	483(3)	0.78(10)	35.6
	$Zn_xFe_{3-x}O_4$ (ii)	0.66(16)	0.27(33)	483(3)	0.73(12)	29.0
	$\delta-Zn_xFe_{1-x}OOH$	0.54(2)	0.00(3)	522(2)	0.45(8)	12.4

*mode of the distributed hyperfine magnetic fields (DHMF)

Table 3 Mössbauer parameters obtained at 293 K and 7 K for S37 synthesized with a Zn/Fe molar ratio of 3/7

Temperature K	Component	δ mm s^{-1}	ΔEq mm s^{-1}	H kOe	Γ mm s^{-1}	Yields %
293	$\delta-Zn_xFe_{1-x}OOH$	0.36(1)	0.76(2)		0.66(3)	100
7	$\delta-Zn_xFe_{1-x}OOH$ (i)	0.46(2)	−0.07(3)	477(1)	0.70(6)	37.6
	$\delta-Zn_xFe_{1-x}OOH$ (ii)	0.50(1)	0.01(2)	519(1)	0.75(4)	62.4

spinel structure, respectively [11, 12], and a component with DHMF corresponds to the surface or defects of the nanoparticles (Fig. 4b). The number of B sites is twice as large as the number of A sites in the spinel Fe_3O_4 structure, and the number of Zn in A and B sites of $Zn_xFe_{3-x}O_4$ can be estimated by the areal intensities of the A and B sites in the Mössbauer spectra. In the $Zn_xFe_{3-x}O_4$ sample S64, the areal intensity of B sites (29.0%) was smaller than that of A sites (49.5%), which suggests that Zn^{2+} preferentially occupies B sites, and the areal intensity ratio of A sites to B sites was calculated to be $A_{Fe}/B_{Fe} = 1.7$.

Mössbauer spectra of S55 acquired at 293 and 14 K are shown in Fig. 5a, and the parameters are summarized in Table 2. The spectrum acquired at 293 K showed a superparamagnetic doublet. The Mössbauer spectrum at 14 K showed three sets of sextets and a component with DHMF. Two sextets, i and ii, correspond to the A and B sites of the zinc spinel structure of $Zn_xFe_{3-x}O_4$, respectively, and another sextet corresponds to δ-FeOOH. A component with DHMF was assigned to the surface or defects of the nanoparticles (Fig. 5b). The difference in the areal intensities of A (35.6%) and B (29.0%) sites was smaller than that for S64, and the areal intensity ratio of Fe in A and B sites was calculated to be $A_{Fe}/B_{Fe} = 1.2$. As the amount of Zn atoms substituted on B sites became small in S55, the area intensity of the B site became larger than that for S64.

Figure 6 shows Mössbauer spectra of S37 acquired at 293 and 7 K, and the parameters are summarized in Table 3. The spectrum acquired at 293 K showed a superparamagnetic doublet. The Mössbauer spectrum at 7 K had two sextets with similar parameters to those for δ-FeOOH reported in our previous work [7]. The component with a smaller hyperfine magnetic field corresponds to the surface or defects of the nanoparticles, and the component with the larger hyperfine magnetic field corresponds to the core Fe atoms of the δ-FeOOH nanoparticles.

Table 4 Compositional formulae for all the samples

Sample(Zn/Fe)	Compositional formula
7/3	$Zn_{0.689}Fe_{2.311}O_4$
6/4	$Zn_{0.628}Fe_{2.372}O_4$
5/5	$Zn_{0.427}Fe_{2.573}O_4$
	$\delta - Zn_{0.142}Fe_{0.858}OOH$
4/6	$Zn_{0.286}Fe_{2.714}O_4$
	$\delta - Zn_{0.095}Fe_{0.905}OOH$
3/7	$\delta - Zn_{0.056}Fe_{0.944}OOH$

We have previously reported the synthesis of δ-FeOOH nanoparticles by the rapid oxidation of Fe_3O_4 [7]. Zn-doped feroxyhyte (δ-$Zn_xFe_{1-x}OOH$) was similarly considered to be formed when divalent iron (Fe^{2+}) in $Fe^{II}Fe_2^{III}O_4$ is rapidly oxidized to trivalent iron (Fe^{3+}). We have also reported the synthesis of copper ferrite nanoparticles using a solution of $FeCl_2$ and $CuSO_4$ as starting materials in the presence of gelatin, in which approximately 80% of the Fe^{2+} was substituted by Cu^{2+} in a precursor magnetite [8]. In the present case, Zn^{2+} ions were doped into iron oxide and formed $Zn_x^{II}Fe_{1-x}^{II}Fe_2^{III}O_4$. The compositional formulae of the five samples were estimated from the molar ratios of Zn/Fe measured using ICP and are summarized in Table 4. S73 ($Zn_{0.689}Fe_{2.311}O_4$) and S64 ($Zn_{0.628}Fe_{2.372}O_4$) maintained the zinc ferrite structure $Zn_x^{II}Fe_{1-x}^{II}Fe_2^{III}O_4$, which prevented further oxidation of the nanoparticles. When the amount of Zn doping was decreased (S55 and S46), δ-$Zn_xFe_{1-x}OOH$ appeared due to rapid oxidation of Fe^{2+} in $Zn_x^{II}Fe_{1-x}^{II}Fe_2^{III}O_4$. S37 ($\delta$-$Zn_{0.056}Fe_{0.944}OOH$) was completely oxidized into δ-$Zn_xFe_{1-x}OOH$ while rinsing under the ambient atmosphere.

4 Conclusions

Zinc-iron oxide nanocomposites were successfully synthesized by the room temperature chemical reaction of $ZnCl_2$ and $FeCl_2$ in the presence of gelatin. The composition of the products could be controlled by variation of the Zn/Fe mixture ratios in the starting materials. Zn-doped feroxyhyte δ-$Zn_xFe_{1-x}OOH$ nanoparticles were obtained when the Zn/Fe ratio was less than 3/7, and $Zn_xFe_{3-x}O_4$ became more dominant with an increase in the Zn/Fe ratio. δ-$Zn_xFe_{1-x}OOH$ nanoparticles were formed by the rapid oxidation of Fe^{2+} in the $Zn_x^{II}Fe_{1-x}^{II}Fe_2^{III}O_4$ precursor. $Zn_xFe_{3-x}O_4$ nanoparticles were spherical with diameters of ca. 10 nm, and δ-$Zn_xFe_{1-x}OOH$ particles were needle-like with around lengths of ca. 100 nm.

References

1. Liu, X., Liu, J., Zhang, S., Nan, Z., Shi, Q.: Structural, magnetic, and thermodynamic evolutions of Zn-doped Fe_3O_4 nanoparticles synthesized using a one-step solvothermal method. J. Phys. Chem. C. **120**, 1328–1341 (2016)
2. Zhu, J., Nan, Z.: Zn-doped Fe_3O_4 nanosheet formation induced by EDA with high magnetization and an investigation of the formation mechanism. J. Phys. Chem. C. **121**, 9612–9620 (2017)
3. Liu, J., Bin, Y., Matsuo, M.: Magnetic behavior of Zn-doped Fe_3O_4 nanoparticles estimated in terms of crystal domain size. J. Phys. Chem. C. **116**, 134–143 (2012)

4. Schwertmann, U., Cornell, R.M.: Iron Oxides in the Laboratory: Preparation and Characterization. Wiley-VCH Weinheim, Germany (2000)
5. Polyakov, A.Y., Goldt, A.E., Sorkina, T.A., Perminova, I.V., Pankratov, D.A., Goodilin, E.A., Tretyakov, Y.D.: Constrained growth of anisotropic magnetic δ-FeOOH nanoparticles in the presence of humic substances. CrystEngComm **14**, 8097–8102 (2012)
6. Pereira, M.C., Garcia, E.M., Silva, A.C., Lorencon, E., Ardisson, J.D., Murad, E., Fabris, J.D., Matencio, T., Ramalho, T.C., Rocha, M.V.J.: Nanostructured δ-FeOOH: a novel photocatalyst for water splitting. J. Mater. Chem. **21**, 10280–10282 (2011)
7. Nishida, N., Amagasa, S., Kobayashi, Y., Yamada, Y.: Synthesis of superparamagnetic δ-FeOOH nanoparticles by a chemical method. Appl. Surf. Sci. **387**, 996–1001 (2016)
8. Nishida, N., Amagasa, S., Kobayashi, Y., Yamada, Y.: One-pot production of copper ferrite nanoparticles using a chemical method. Hyperfine Interact. **237**, 111 (2016)
9. Rubinstein, M., Forester, D.W.: Investigation of the insulating phase of magnetite by NMR and the Mössbauer effect. Solid State Commun. **9**, 1675–1679 (1971)
10. Ito, A., Ono, K., Ishikawa, Y.: A study of the low temperature transition in magnetite. J. Phys. Soc. Jpn. **18**, 1465–1473 (1963)
11. Li, Y.H., An, S.Y., Kim, C.S.: Study of site occupancy in $Zn_xFe_{3-x}O_4$ microspheres based on Mössbauer analysis. IEEE. T. MAGN. **49**, 7 (2013)
12. Ferrari, S., Aphesteguy, J.C., Saccone, F.D.: Structural and magnetic properties of Zn-doped magnetite nanoparticles obtained by wet chemical method. IEEE. T. MAGN. **51**, 6 (2015)